

DESY SR 86-12
December 1986

BOUND-FREE FLUORESCENCE OF RARE GAS HYDRIDES

by

T. Möller, M. Beland, G. Zimmerer

II. Institut f. Experimentalphysik, Universität Hamburg

Eigentum der	DESY	Bibliothek
Property of		Library
Zugang:	12. JAN 1987	
Accession:		
Leihfrist:	7	7
Loan period:		days

ISSN 0723-7979

NOTKESTRASSE 85 · 2 HAMBURG 52

DESY behält sich alle Rechte für den Fall der Schutzrechtserteilung und für die wirtschaftliche Verwertung der in diesem Bericht enthaltenen Informationen vor.

DESY reserves all rights for commercial use of information included in this report, especially in case of filing application for or grant of patents.

To be sure that your preprints are promptly included in the
HIGH ENERGY PHYSICS INDEX ,
send them to the following address (if possible by air mail) :

DESY
Bibliothek
Notkestrasse 85
2 Hamburg 52
Germany

BOUND-FREE FLUORESCENCE OF RARE GAS HYDRIDES

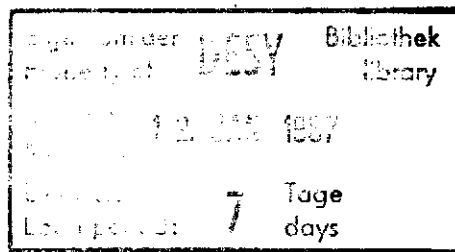
Thomas Müller, Michael Beland and Georg Zimmerer

II. Institut für Experimentalphysik, Universität Hamburg,
D-2000 Hamburg 50, FRG

Abstract

Bound-free fluorescence of HeH, NeH, ArH, KrH and XeH is reported. The excimers are formed in a photochemical reaction between H_2 ($C^1\Pi_u$, $B^1\Sigma_u^+$) and rare gases using synchrotron radiation for the excitation of H_2 . Broad fluorescence continua in the near UV are observed and assigned to the rare gas hydride transition $B^2\Pi + X^2\Sigma^+$. In the case of NeH, also the $A^2\Sigma^+$ seems to contribute to the fluorescence spectrum. Experimentally derived binding energies of the B-state and bound-free spectra of HeH and ArH are in a good agreement with recently performed ab initio calculations. Radiative lifetimes, quenching cross sections and formation cross-sections are determined.

submitted to Chem. Phys. Letters



1. Introduction

During the last decade, numerous investigations of excimer molecules have been carried out because excimers have outstanding properties in high power UV laser [1]. Rare gas hydrides, especially HeH, are very simple excimers with strongly bound excited states which were predicted in 1963 by Michals and Harris [2] and confirmed in a beam experiment of Gray and Tomlinson [3] and in more recent calculations [4 and references therein]. Two different aspects are of special interest,

- (i) the electronic properties and decay mechanisms of the excited states, and
- (ii) formation of the hydrides.

With the exception of ArH [5,6], gas discharges in mixtures of H_2 and rare gases are very inefficient to produce rare gas hydrides [7]. Therefore, radiative transitions of, e.g., HeH and NeH could be observed only recently using advanced techniques. By irradiating a mixture of H_2 and He with synchrotron radiation, we were able to observe a bound-free continuum of HeH which was attributed to the transition $B^2\Pi + X^2\Sigma^+$ [8] (notation after [4]). Discrete molecular spectra of isotopically pure HeH and NeH were observed by Ketterle et al. [9] in a beam experiment. Brooks et al. [10] demonstrated that HeH can be formed at the interface of solid hydrogen and dense He gas under bombardment with fast protons. Recently, Lipschitz [11] reported discrete molecular spectra of XeH in an especially designed penning excitation source. In our work on HeH we proposed that the lowest bound state $A^2\Sigma^+$ is predissociated by the ground state $X^2\Sigma^+$, similarly as Johns reported for ArH [5]. In the meantime, the rate of predissociation of HeH was clarified experimentally using fast beam techniques [12,13,14]. The competition between radiative and nonradiative transitions was also calculated by van Hemert et al. [15] making use of the ab initio calculations of the potential energy curves performed by Dohmann et al. [16]. In summing up the efforts for a better understanding of the properties of rare gas hydrides, we finally want to mention the trajectory calculation of formation cross section for HeH in H_2^+-He reactive collisions performed by Farantos et al. [17].

In an extension of our earlier work [8], in this paper bound-free fluorescence spectra of all rare gas hydrides are presented. The molecules were formed in a photochemical reaction of the type



(Rg = He, Ne, Ar, Kr, Xe). For this purpose, gas mixtures of H_2 and the rare gases were excited selectively with synchrotron radiation. In this way, the excitation spectra of the RgH emission could be measured. From the energetical onset of the excitation spectra, the binding energies of the excited states involved could be deduced. Formation cross sections were obtained from a comparison of H_2 and RgH fluorescence. Exploiting the time structure of synchrotron radiation, lifetime measurements were performed. They are helpful for a safe assignment of the broad bound-free continua. For KrH and XeH, only a few preliminary experiments were carried out.

2. Experiment

The measurements were carried out at the experimental station SUPERLUMI at HASYLAB, Hamburg. The experimental arrangement has been described elsewhere [18,19]. Spectrally selected synchrotron radiation was used to excite gas mixtures of 0-5 torr H_2 and 1-30 torr rare gas enclosed in a gas cell. For excitation wavelengths below 104 nm this cell was equipped with thin (thickness 100 nm) indium windows. The fluorescence light was analysed perpendicular to the exciting beam with a band pass of 10 nm. The signal-to-noise ratio was improved by exploiting the time structure of synchrotron radiation. Fluorescence was recorded only within a short time window (≈ 10 ns) immediately following the excitation pulse (fwhm = 150 ps, repetition rate 1 MHz). The length of the time window roughly corresponds to the lifetime of the emitting state. Typical counting rates are 10-100 cps for the fluorescence spectra.

Excitation spectra and decay curves were measured with the aid of a photomultiplier directly connected with the gas cell. In this way, counting rates up to 10^4 cps were obtained. The pressure dependent decay rates were evaluated from the measured decay curves with a deconvolution procedure.

3. Results and Discussion

3.1 Formation of the Rare Gas Hydrides and Fluorescence Spectra

Fig. 1 shows the calculated potential energy curves of HeH [4] and of H_2 [20] which are of importance in the context of this paper. The pathway of the photochemical reaction (1) is indicated by arrows. By an appropriate choice of the excitation wavelength, rotationally selective primary excitation of the B-state or the C-state of H_2 is achieved. For the chosen excitation wavelengths, only the A and the B state of HeH are accessible. Though Fig. 1 is valid only for HeH, it should also hold schematically for NeH and ArH due to the great similarities between their potential energy curves [4]. Concerning KrH and XeH, no potential energy curves are available, but with respect to the ground state of the molecular ions, KrH^+ and XeH^+ [21,22], strongly bound excimer states are expected, too.

In Fig. 2 we present the bound-free fluorescence spectra of the rare gas hydrides. They were obtained at room temperature from mixtures which consisted of 20 torr Rg and .3 torr H_2 . In the case of HeH, NeH, and ArH the excitation wavelengths given in Fig. 2 are near to the energetical threshold of reaction (1). Therefore, the spectra most probably stem from the lowest vibrational level of the emitting excimer state. The thresholds were determined from the excitation spectra (see Sec. 3.2). Near threshold excitation was not possible for KrH and XeH because of low counting rates. Therefore, the KrH and XeH spectra presented in Fig. 2 most probably contain contributions from more than one vibration level.

In Fig. 3, the fluorescence spectra of NeH are presented for various excitation wavelengths. These wavelengths correspond to primary excitation of the vibrational levels $v' = 2 \dots 5$ of $\text{H}_2 \text{C } ^1\Pi_u$. The fluorescence maximum shifts to shorter wavelengths with increasing photon energy of excitation. This behaviour shows that more and more also higher vibrational levels of the emitting excimer states are populated in reaction (1). The higher levels preferably emit at shorter wavelengths. Similar results were obtained for the other rare gas hydrides [23].

3.2 Excitation Spectra and Threshold Energies

Fig. 4 shows excitation spectra of near UV and visible fluorescence of H_2 and of mixtures of H_2 and rare gases. The resolution interval of 0.05 nm is sufficiently small to resolve single rotational levels of $H_2 C^1\Pi_u$ or $B^1\Sigma_u^+$ states. In pure H_2 only lines of a contamination of N_2 (≤ 200 ppm) are observed [8]. In the presence of rare gases the rovibronic structures of the $C^1\Pi_u$ and $B^1\Sigma_u^+$ of H_2 appear, but with different threshold energies for each hydride. These energies correspond to the energetical threshold of reaction (1). If we assume a dissociation of the excimers into $Rg(1S_0) + H(2s, 2p)$ we are able to determine the dissociation energies of the excimer states from the energy of the threshold and the well known dissociation energy of H_2 [20]. In our first paper [8] as an approximation of the threshold, the energetically lowest band in the excitation spectra was taken.

In an improved model, we now take into account endothermic reactions with an energy defect, ΔE , which has to be overcome by translational energy of the collision partners. We suppose, that the efficiency of vibrational and translational energy for the formation near the threshold of reaction (1) is comparable. Then the energy defect ΔE should be correlated with the intensity ratio of neighbouring vibrational levels of H_2 in the excitation spectra just below and above the threshold in a simple way:

$$I(v'-1)/I(v') = \sigma(v'-1)/\sigma(v') = \sqrt{\Delta E/kT} \exp(-\Delta E/kT) \quad (2)$$

Here $\sigma(v'-1)$ and $\sigma(v')$ are the formation cross sections of reaction (1) just below and above the threshold, and kT is the Boltzmann factor. Relation (2) is derived from simple gas kinetic expressions. From the thus deduced threshold energies the binding energies of the excimer states are obtained by adding the energies of the zero point motion (1500 cm^{-1}) which were estimated from the molecular ions [24]. The binding energies are collected in Table 1 and compared with calculated values (A state and B state). In the case of HeH and ArH, the experimental results agree well with the theoretical binding energies of the B states. This is one of the reasons why we assigned the fluorescence to $B + X$ transitions. In the case of NeH, good agreement is found for the A-state. Details are discussed below.

From the intensity ratio of H_2 and rare gas hydride fluorescence, the cross sections of reaction (1) were deduced [23]. They range between 1 \AA^2 and 25 \AA^2 . They are in qualitative agreement with the results of Farantos [17]. In general, formation via $H_2 C^1\Pi_u$ is more efficient than via $B^1\Sigma_u^+$. Details will be discussed elsewhere.

3.3 Lifetimes and Quenching Cross Sections

For HeH, NeH and ArH, the decay rates of the fluorescence spectra were measured as a function of gas pressure p . With an excitation bandwidth of 0.25 nm, only a few rotational levels ($J' \leq 3$) of the $H_2 C^1\Pi_u$ precursor states are populated. Fig. 5 shows the decay rates of HeH $B^2\Pi$, ($v' = 0$) $\rightarrow X^2\Sigma^+$ as a function of pressure. The data can be fitted with

$$K = K_{\text{rad}} + k_Q \cdot p \quad (3)$$

With an extrapolation to $p = 0$, a radiative decay rate $K_{\text{rad}} = 5.6 \times 10^7 \text{ s}^{-1}$ corresponding to $\tau_{\text{rad}} = (18 \pm 4) \text{ ns}$ is obtained. The quenching rate constant is $2.7 \times 10^{-10} \text{ cm}^3 \text{ s}^{-1}$ corresponding to a quenching cross section of 17 \AA^2 . The results are in good agreement with another recent experimental value of $(18 \pm 1) \text{ ns}$ [12] as well as with the calculated lifetime of the B-state (19 ns) [26].

The decay rates of NeH and of ArH depend on the excitation wavelength indicating that different electronic states are involved in the decay dynamics. Some preliminary results have already been presented [27]. A detailed investigation is in progress now [25].

3.4 The Assignment of the Bound-Free Fluorescence Spectra

The bound-free continuum of HeH has already been assigned to the transition $B^2\Pi \rightarrow X^2\Sigma^+$ [8]. Some of the arguments are given again in this paper. In the meantime, our assignment has been established in different beam experiments [12,13,14]. The assignment is corroborated by comparing the experimental spectrum with a calculated spectrum [26] making use of ab initio calculations of potential energy curves [16]. Very good agreement between experiment and theory is found (Fig. 6). Fig. 6 includes also a

comparison for ArH which is satisfactory, too. In view of the good agreement of the experimental and calculated threshold energies, the ArH continuum (at threshold excitation) has to be assigned to B \rightarrow X transition, too.

In principle, we could also expect the formation of the excimers in the A $^2\Sigma^+$ state. In HeH and ArH, no fluorescence of the A states was observed, since they are predissociated by the $^2\Sigma^+$ groundstate [5,13]. For NeH, however, the situation is not so clear. A comparison between the calculated binding energy of the B state [4] and the experimentally determined value (see Table 1) yields a deviation of $\approx .3$ eV. At first it seemed as if the values calculated by Theodorakopoulos et al. [4] were too small like in the case of ArH. More sophisticated calculations of Dohmann removed the discrepancy in the case of ArH [16] but confirmed the results for NeH [26].

The variation of the radiative lifetime of the NeH continuum with excitation energy (see Sec. 3.3) is an indication that two different electronic states emit. A calculation of predissociation rates, which sensitively depend on the radial coupling between the states involved, or beam experiments similar to the study of van der Zande et al. [13] and Peterson et al. [14] are highly desirable to clarify the situation.

In the case of KrH and XeH only a comparison with binding energies of the molecular ions KrH $^+$ and XeH $^+$ is possible. The tendency of increasing binding energy for the heavier rare gases is established [24]. However, on the basis of the preliminary results available so far, a safe assignment of the observed emission to either the A or the B state is not possible.

Acknowledgment

We want to thank Dr. H. Dohmann (University of Bonn) who made us available the results of his calculations prior to publication and who participated with many helpful discussions. The work was supported by the Bundesminister für Forschung und Technology (BMFT) of the Federal Republic of Germany.

Figure Captions

Figure 1

Potential curves of selected states of HeH and H $_2$. Data are taken from Ref. 4 and Ref. 20. The excitation of H $_2$ is indicated by an arrow. The horizontal line makes clear the reaction pathway. The HeH transition which is responsible for the broad UV-continuum is indicated by an arrow, too.

Figure 2

Bound-free fluorescence of rare gas hydrides obtained at gas pressures of typically 0.3 torr H $_2$ and 20 torr rare gas. The excitation wavelength are given in the figure.

Figure 3

Bound-free fluorescence of NeH as a function of excitation wavelength. Experimental conditions are the same as in Fig. 2.

Figure 4

Excitation spectra of near UV and visible fluorescence of H $_2$ and H $_2$ /rare gas mixtures. Band heads of the transition H $_2$ X $^1\Sigma_g^+$ \rightarrow B $^1\Sigma_u^+$ or C $^1\Pi_u$ are indicated.

Figure 5

Decay rate of HeH B $^2\Pi$ ($v'=0$) \rightarrow X $^2\Sigma^+$ as a function of pressure.

Figure 6

UV fluorescence of HeH following primary excitation of H $_2$ C $^1\Pi_u$ ($v'=2$) and ArH following primary excitation of Ar 3P_1 at 106.6 nm in comparison with calculated spectra [15,26].

Table 1

Comparison between experimental and calculated binding energies of rare gas hydrides. a: taken from Ref. 4; b: taken from Refs. 16, 26.

	HeH	NeH	ArH	KrH	XeH
D_0 [eV]					
this work	2.19±0.03	1.96±0.03	3.11±0.03	3.19±0.05	≥ 3.5
theory					
$B \ ^2\Pi$	2.20 ^a 2.16 ^b	1.67 ^a 1.70 ^b	2.88 ^a 3.18 ^b		
$A \ ^2\Sigma^+$	2.49 ^a 2.49 ^b	1.91 ^a 1.93 ^b	3.73 ^a 3.80 ^b		

References

1. C.K. Rhodes, Excimer Lasers, Topics in Appl. Physics, 2. Edition, Springer, New York 1984
2. H.H. Michels, F.E. Harris, J. Chem. Phys. 39, 1464 (1963)
3. J. Gray, R.H. Tomlinson, Chem. Phys. Lett. 4, 251 (1969)
4. G. Theodorakopoulos, S.C. Farantos, R.J. Buenker, S.D. Peyerimhoff, J. Phys. B: At. Mol. Phys. 17, 1453 (1984)
5. J.W.C. Johns, J. Mol. Spectr. 36, 488 (1970)
6. C.R. Lishawa, J.W. Feldstein, T.N. Stewart, E.E. Muschlitz Jr., J. Chem. Phys. 83, 133 (1985)
7. A. Kunde, N.J. Wiegart, H.J. Kunze, J. Phys. B: At. Mol. Phys. 18, 567 (1985)
8. T. Möller, M. Beland, G. Zimmerer, Phys. Rev. Lett. 55, 2145 (1985)
9. W. Ketterle, H. Figger, H. Walther, Phys. Rev. Lett. 55, 2941 (1985)
10. R.L. Brooks, J.L. Hunt, J.J. Miller, Phys. Rev. A (1986), in print
11. R.H. Lipson, Chem. Phys. Lett. 129, 82 (1986)
12. W. Ketterle, A. Dodhy, H. Walther, Chem. Phys. Lett. 129, 76 (1986)
13. W.J. van der Zande, W. Koot, D.P. Bruijn, C. Kubach, Phys. Rev. Lett. 57, 1219 (1986)
14. J.R. Peterson, Y.K. Bae, Phys. Rev. A (1986), in press
15. M. van Hemert, H. Dohmann, S.D. Peyerimhoff, Chem. Phys., in press
16. H. Dohmann, P.J. Bruna, A. Nigge, S.D. Peyerimhoff, to be published
17. S.C. Farantos, to be published
18. H. Wilcke, W. Böhmer, N. Schwentner, Nucl. Instr. Meth. 208, 59 (1983)
19. P. Gürtler, E. Roick, G. Zimmerer, M. Pouey, Nucl. Instr. Meth. 208, 835 (1983)
20. T.E. Sharp, Atomic Data 2, 119 (1971)
21. P. Rosmus, E.A. Reinsch, Z. Naturforsch. 35a, 1066 (1980)
22. H.U. Mittmann, H.P. Weise, A. Ding, A. Henglein, Z. Naturforsch. 26a, 1112 (1971)
23. T. Möller, Ph.D. thesis, Hamburg (1986)
24. R. Klein, P. Rosmus, Z. Naturforsch. 39a, 349 (1984)
25. M. Joppien, T. Möller, G. Zimmerer, to be published
26. H. Dohmann, private communication
27. T. Möller, M. Beland, G. Zimmerer, VUV-8, Vacuum Ultraviolet Radiation Physics, Lund (Sweden) 1986, Book of Abstracts, p. 230

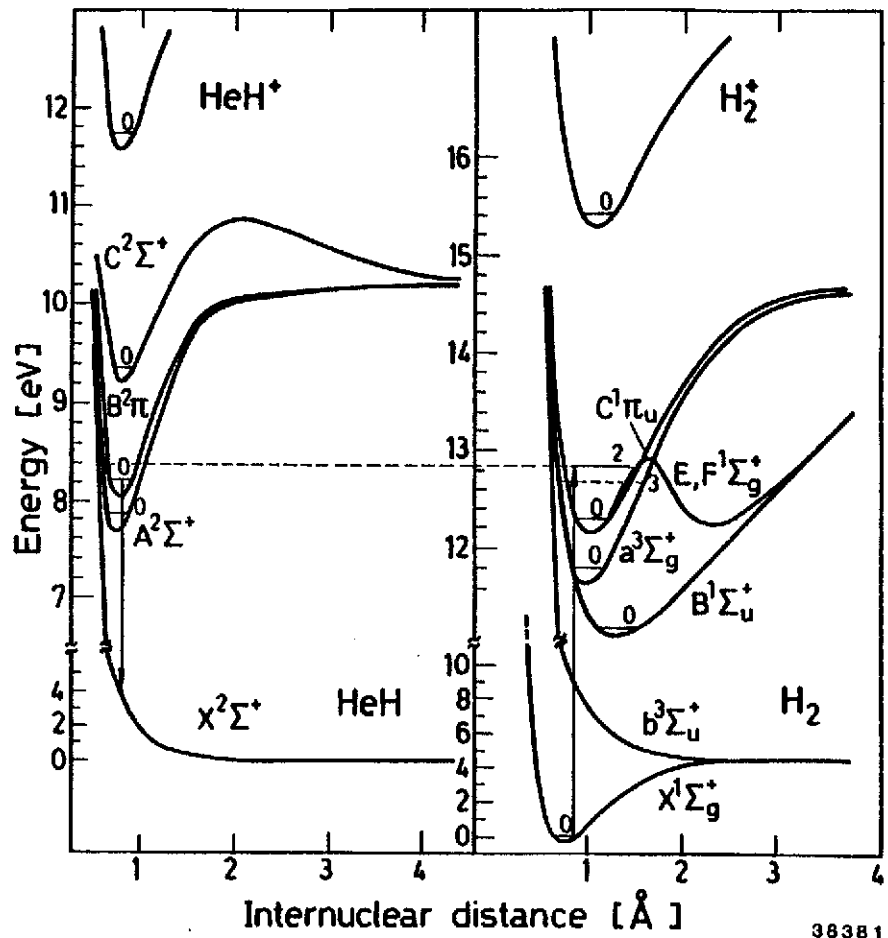


Fig. 1

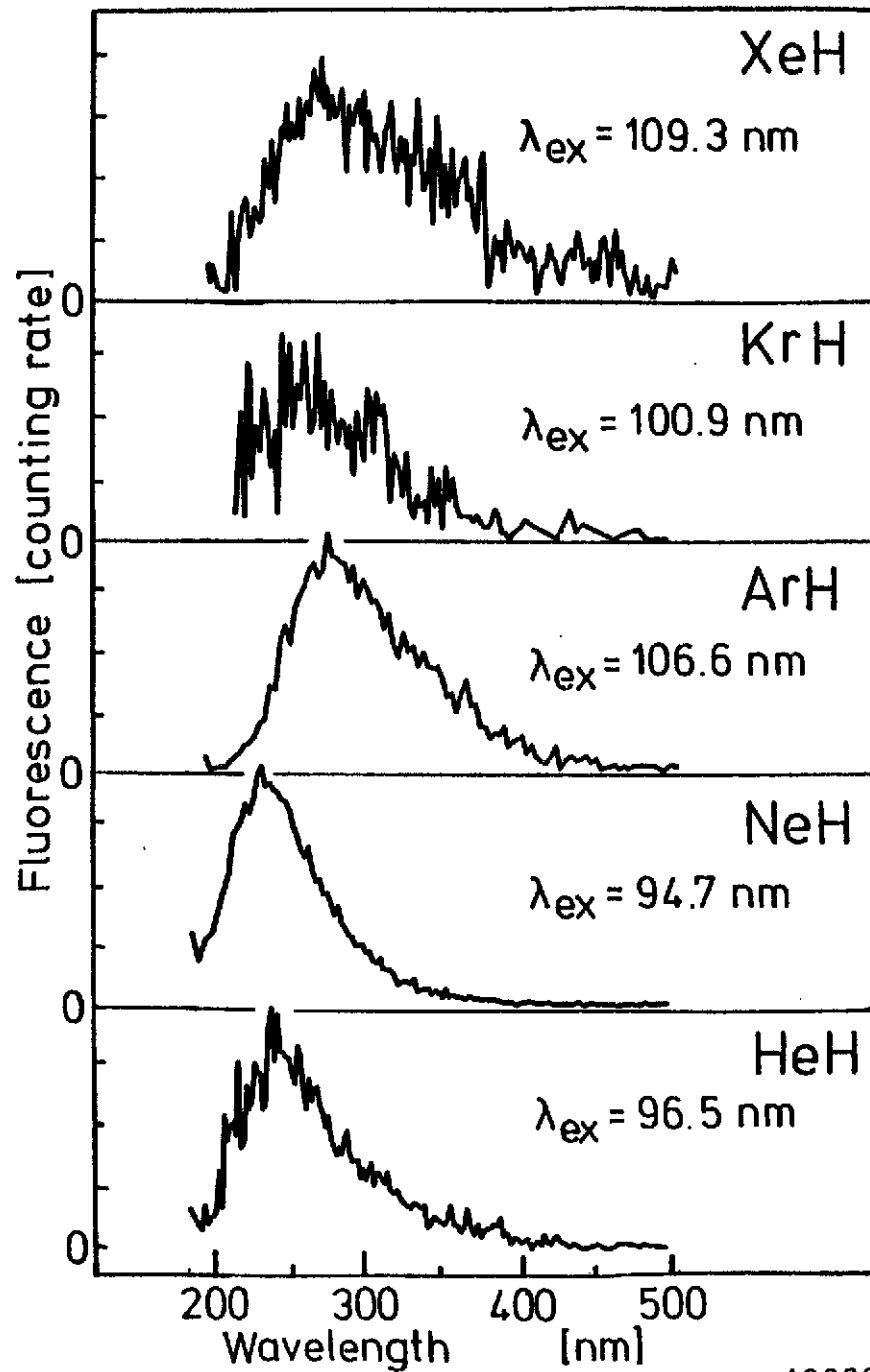


Fig. 2

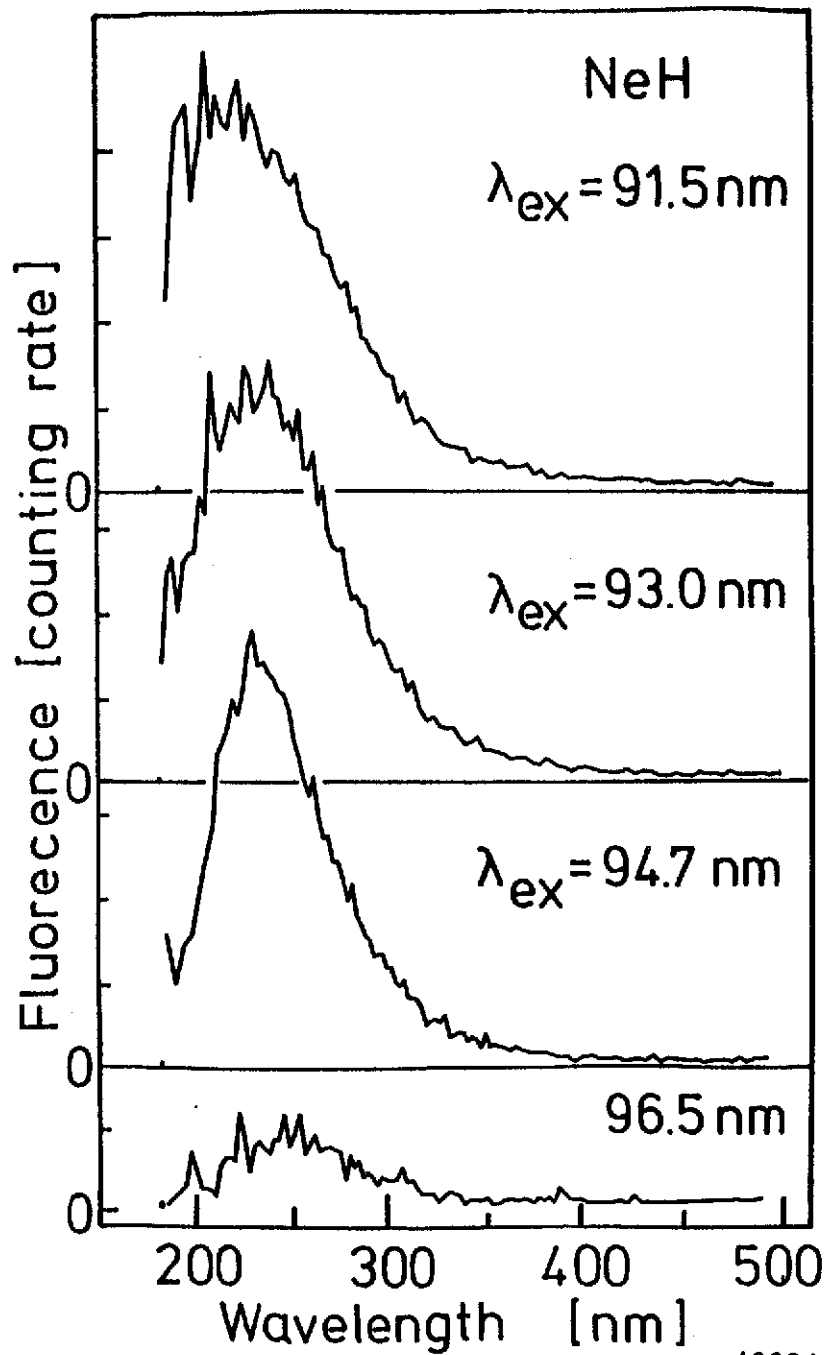


Fig. 3

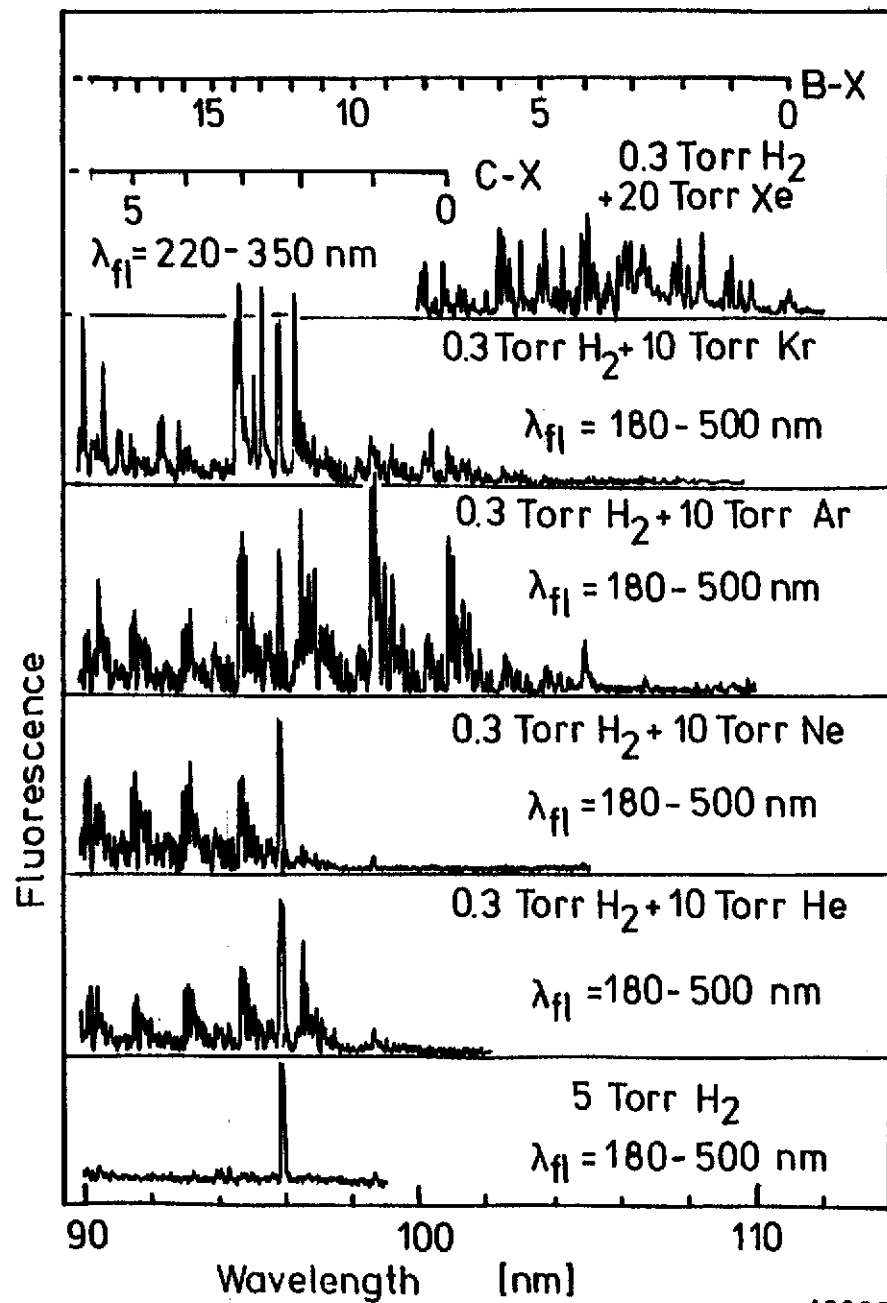


Fig. 4

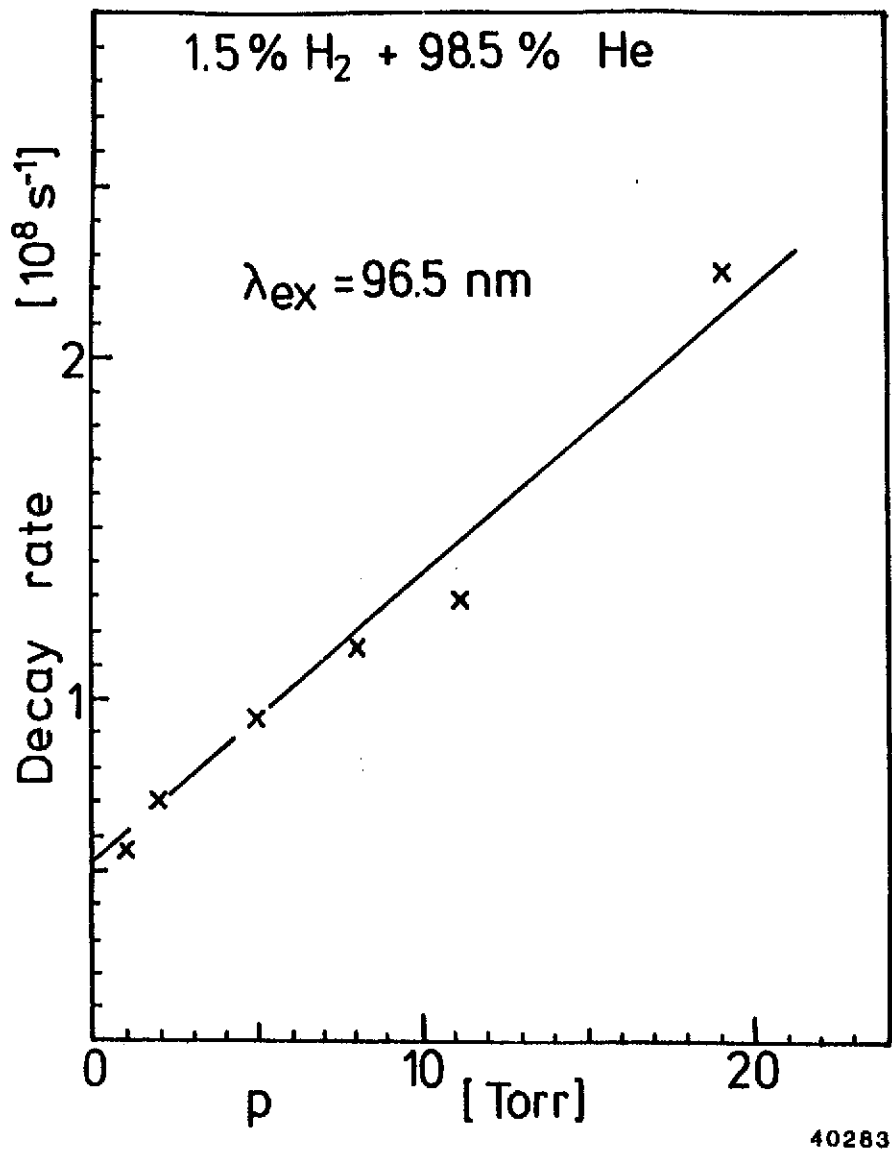


Fig. 5

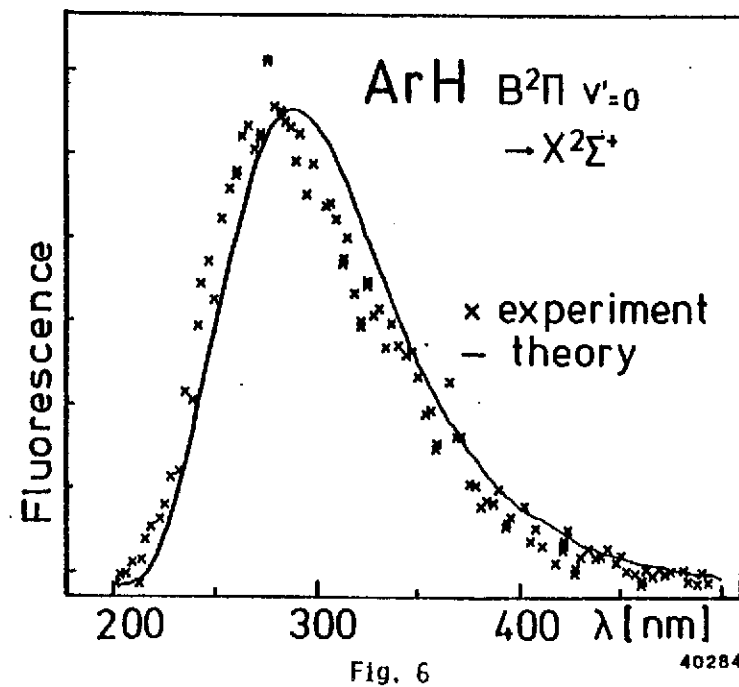
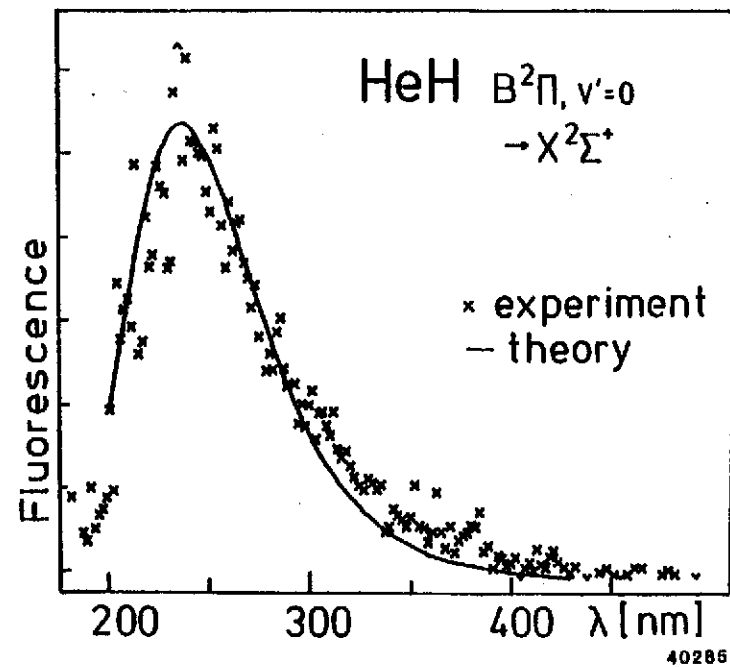


Fig. 6